Correlation of spatial intensity distribution of light reaching the retina and restoration of vision by optogenetic stimulation

Shivaranjani Shivalingaiah[1, 2], Ling Gu[1], Samarendra K. Mohanty[1]

[1]Department of Physics; [2]Department of Biomedical Engineering,
University of Texas, Arlington, TX 76019.

ABSTRACT

Stimulation of retinal neuronal cells using optogenetics via use of chanelrhodopsin-2 (ChR2) and blue light has opened up a new direction for restoration of vision with respect to treatment of *Retinitis pigmentosa* (RP). In addition to delivery of ChR2 to specific retinal layer using genetic engineering, threshold level of blue light needs to be delivered onto the retina for generating action potential and successful behavioral outcome. We report measurement of intensity distribution of light reaching the retina of Retinitis pigmentosa (RP) mouse models and compared those results with theoretical simulations of light propagation in eye. The parameters for the stimulating source positioning in front of eye was determined for optimal light delivery to the retina. In contrast to earlier viral method based delivery of ChR2 onto retinal ganglion cells, *in-vivo* electroporation method was employed for retina-transfection of RP mice. The behavioral improvement in mice with Thy1-ChR2-YFP transfected retina, expressing ChR2 in retinal ganglion cells, was found to correlate with stimulation intensity.

Key words: Retinitis Pigmentosa, Optogenetics, Electroporation, Retinal prosthesis, Optical imaging

1. INTRODUCTION

Vision is an essential component of human health that has physical, emotional as well as psychological importance in everyday life. Retinitis pigmentosa (RP) refers to disorders characterized by degeneration of photoreceptors in the eye which hinders visual ability by non functional neuronal activation and transmission of signals to the cortex[1,2]. The prevalence of this disease is at least one million individuals[2]. The disease is most often inherited as an autosomal recessive trait with large number of cases having this form of inheritance [2, 3]. Although genetic testing is available for RP, it may not be sufficient to assess the risk of passing the disorder from parent to offspring, and even proactive approaches may not be sufficient to prevent its occurrence[2, 4]. Most of the current clinical treatments are primarily focused on slowing down the progression of the disease, as there is neither any cure that can stop the disease nor any therapy that can restore any vision lost due to this disease[5]. The current treatment modality for partial restoration of vision is highly invasive involving surgical procedure for retinal Implants/transplants. While subretinal implants[6,7] suffers from the disadvantages of damage to the device over a period of time, and microphotodiode not being able to produce a sufficient current to stimulate adjacent neurons with the use of ambient light; the epiretinal implants[7,8] lead to cellular proliferation due to surgical implantation of the device, and disordered stimulation pattern resulting from the electrical stimulation of both the axons and cell bodies of the ganglion cells[7]. Besides being highly invasive in nature, all these existing methods for restoration of vision are based on non-specific cellular activation and have low spatial resolution, and hence have not been very successful in restoration of vision.

Recent advent[9] of optical stimulation of genetically targeted neurons "Optogenetics" has several advantages over electrical stimulation such as cellular specificity and mechanical non-invasiveness. Now, chemically identical neurons[10] can be activated by blue light with high temporal precision by introducing a light-activated molecular channel, named channelrhodopsin-2 (ChR2), into specific groups of cells by genetic targeting[10-12]. Since ChR2 is a non-selective cation channel, light-induced activation of ChR2 results in depolarization of only those neurons that express ChR2. Selective activation of neurons by ms-pulsed blue light has been demonstrated in cell culture, brain slices, as well as in small animals[13,14]. Since very low intensity (few mW/ mm^2) light is required for optogenetic stimulation, it has translational

potential, especially in sensitizing photo-degenerated retina. While the recent studies using non-specific transfection of retina [15] as well as promoter-specific targeting of retinal ganglion cells using viral method provided contradictory behavioral results[16, 17], targeting ON-bipolar cells using *in-utero* electroporation[18] led to improvement of visual function. The disparity between these results could arise due to differences in expression level and or light intensity reaching the retina not being sufficient to activate ChR2-sensitized cells. In addition to delivery of ChR2 to specific retinal layer using genetic engineering, threshold level of blue light needs to be delivered onto the retina for generating action potential and successful behavioral outcome. Here, we report measurement of intensity distribution of light reaching the retina of RP mouse models and comparison with theoretical simulations of light propagation in eye based on optical system design software. In contrast to earlier viral method based delivery of ChR2 onto retinal ganglion cells, *in-vivo* electroporation method was employed for retina-transfection of RP mice. The irradiance requirement to achieve optimal improvement in behavioral responses after transfection of CHR2 was found to correlate with theoretical estimations.

2. MATERIALS AND METHODS

2.1. Physical optics propagation Method
Zemax, optical system design software was used to model non-image-forming light response for a dark adapted pupil determining minimal source irradiance requirements to achieve sufficient intensity at retina for excitation of ChR2. Zemax modeling of the eye was done in the sequential mode. The lens units were set to millimeter range, and the wavelength was set to "F, d, C (Visible)". Further, one field of type "Angle (Deg)" was set. Three surfaces, namely anterior and posterior corneal surfaces and the aqueous humor are the surfaces defined before the aperture stop (pupil). Anterior and posterior lens surfaces, vitreous humor and the retina are defined after the Pupil stop. Each surface was defined by the parameters, (i) the radius of curvature, (ii) thickness (axial distance of each of the surface from the previous surface), (iii) semi diameter (being the radial thickness) and (iv) refractive index. The spot diagrams are set for 20 rays and the irradiance map was obtained by the physical optics propagation.

2.2. Experimental Animals
Retinal degenerated mice (rd1-rd1 - C57BL/6J-*Pde6b*$^{rd1-2J}$) and C57BL/6 wild type mice were obtained from Jackson laboratory and bred in the animal facilities of the university. Each animal was housed in standard mouse cages under 12 h light/dark cycle. The care and use of the mice was approved by the IACUC committee at University of Texas at Arlington.

2.3. Transfection of CHR2-YFP into rd1/rd1 mouse eyes
As an alternative to viral-based gene transfer, nonviral vectors are easier to prepare and less prone to cause an immunologic reaction. Electroporation is most easily applied to readily accessible tissues such as the eye. Adult (8 weeks old) rd1/rd1 mice were treated humanely in strict compliance with IACUC on the use of animals in research. For transfection of specific layers of retina *in vivo* electroporation was used. ChR2-plasmids with Thy1 promoter to target retinal ganglion cells, and pEYFP was fused for visualization of expression. Before intravitreous injections, mice were anesthetized, pupils were dilated, and a sharpened tip of a sterilized micro-syringe was inserted through the sclera into the vitreous cavity. The injections were carried out with a 32-G needle of a Hamilton micro-syringe to deliver 1 μl of plasmid in each eye, following which the eye was placed within a hemispherical cathode on the cornea and a hemispherical anode with a groove that slides around the optic nerve on the posterior surface of the eye. A function generator was used to deliver variable number of pulses (width: 10 or 50 ms) separated by 100 ms with voltage set at 10 or 5V. The optimal transfection parameters for electroporation were determined by electroporation of HEK cells in suspension with varying parameters like voltage and frequency. The viability of cells after the procedure and efficiency of transfection was evaluated.

2.4. Behavioral assessment
To determine restoration of vision, behavioral testing in water maze task[19] involved determination of score for the mice swimming towards a stimulating light source before and after optogenetic treatment. The mice were divided into 3 groups. Mice in group 1 (control) were trained in the water maze task for duration of 7 days and then tracked twice a week for about 4 weeks. Mice in group 2 were injected with ChR2 construct (Thy1-ChR2-pEYFP), followed by electroporation. Mice in group 2 were trained in the water maze task for a period of 7 days prior to transfection. A removable platform with a diameter of 6 cm and height of 8 cm was suspended into the pool. The maze was then filled with water to a depth of 7 cm at a temperature of 25°C. A weakly diverging laser beam (Rep rate: 10Hz) was directed

into center of the maze forming a 2cm spot at the center. The energy of the laser beam at different distances was measured with a power meter (PM100D, Thorlabs Inc.). One week after injection of plasmids, mice behavior in water maze task was quantified twice a week at varying distances from the light source. Ethovision software was used to analyze the behavior of mice in the pool. Swimming distance, swimming duration, rotation of the head, and number of error arms traveled before finding the platform (light source) were scored for evaluating the ability of the mouse to see the light.

2.5. Measurement of power reaching retina

For power measurements at retina, eyes were extracted from dark adapted mice. The DPSS blue laser beam (473nm, 100mW) was coupled to a 200 µm core optical fiber using a fiber coupler (Newport Inc., USA) and the fiber was positioned at various distances from the cornea surface. The divergence of the beam was similar to that used for behavior test. A receiving fiber having a core diameter of 200µm (area: 0.0314mm^2) was stereotactically inserted from back of the eye to reach the retina surface via a guiding needle. Power from the other end of the receiving optical fiber was measured using a power meter (PM100D, Thorlabs Inc.). The tilt angle of the receiving fiber was adjusted so as to receive the maximum power for each source fiber distance.

2.6. External light source parameters

For the light intensity at the retina to be above the ChR2 stimulation threshold, the light source should have sufficient brightness and optimal divergence so that maximum light can be collected and focused by the cornea-lens on to the retina. Unlike highly-packed pigments in photoreceptors of intact retina which amplifies the signal in cascade, cells expressing ChR2 only on membrane would require orders of magnitude higher light intensity to elicit action potentials. The required photon flux to achieve this depends on the level of ChR2 expression. Assuming maximum ChR2 expression ($2x10^7$ for a cell of diameter 10µm and ChR2 ion channel cross-section ~10nm^2), Grossman et al.[20] have calculated the lower and upper bound for generating action potential to be ~ 0.05 mW/mm^2 and 10mW/mm^2, respectively, for blue light (470 nm). From this threshold cell irradiance required for generating action potential and the transmission characteristics of the eye; one can estimate the required radiance of the external light source.

The source size, its position from the cornea and divergence need to be optimized for getting optimal modulation transfer function of the imaging system (eye). Besides these parameters, the spatial resolution of the restored-vision will depend primarily on the density of ChR2-transfected neuronal cell type. Therefore, spatial resolution will be lower than achieved by the normal retina with tightly-packed natural photoreceptors. Further, it may be comprehended that targeting of higher order neurons with low density such as retinal ganglion cells may provide lower spatial resolution. However, excitation sensitivity of different regions (soma, axon) of one cell and respective processing of the information will contribute to the spatial resolution.

3.   RESULTS AND DISCUSSION

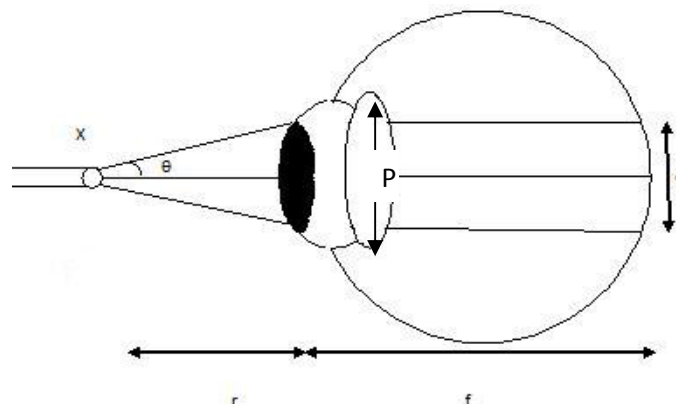### 3.1. Calculation of radiance of source vs. irradiance at mouse retina

Figure 1: *In-vitro* model of a mouse eye being illuminated by a diverging blue light emerging from an optical fiber at a distance (r) from cornea-lens surface. d: The image diameter on the retina; P: pupil diameter; f: the effective focal length of the refracting medium in the eye.

Figure 1 shows an *in-vitro* model of a mouse eye being illuminated by a diverging blue light emerging from an optical fiber (core diameter: 200μm) tip placed at a distance (r) from cornea-lens surface. The image diameter (d) on the retina will depend on the distance of the source (r) and the effective focal length of the refracting medium in the eye (consisting of the cornea, aqueous humor, lens and the vitreous humor) and the size of the source. We consider the source to be a point source (x). The point source at a distance r from the pupil (P) makes a solid angle

$$\Phi = A_P/r^2 = \pi p^2/4r^2 \qquad (1)$$

where A_P is the pupil area and "p" is the pupil diameter. For a dark-adapted mouse[21], the pupil area is 2.29 ± 0.35 mm^2. Thus, the solid angle at a distance of r = 2mm from the pupil is 32.8 degree. The source radiance,

$$L = P_0/ (\Phi A_s \cos\theta) \qquad (2)$$

where P_0 is the total power emitted from the source fiber as measured using a power meter, A_s is area of the source and θ is the half angle. For a source distance r = 2mm, the source radiance L in our experiment was calculated to be L=302.89 mW/(mm^{2}sr). Hence the total power falling on the pupil was calculated as $P = L\Phi A_s = 9.79$ mW. The irradiation power at the retina will therefore be $P_r = \tau P$, where τ is the transmittance of the ocular media for 470nm.

Wavelength	488nm
Cornea	1.4102
Aqueous	1.3390
Vitreous	1.3390
Lens	1.6952

Table 1: Refractive indices at 488nm wavelength

Table 1 lists the refractive indices[22] of the mouse eye at 488 nm, close to the stimulation laser wavelength used in the present study. Using the Fresnel reflectance formula, the reflectance at each layer of the eye (cornea, aqueous humor, lens and the vitreous humor) was calculated. Thus, the transmittance through the above layers up to retina was found to be 0.8688. The area of irradiation at the retina is dependent on the size of the source, divergence and position. At r = 2 mm, the spot size was measured to be 1 mm. Retinal irradiance 'I' is given by P_r/A_r, where A_r is the area of the image at retina. So,

$$I = (\pi\tau /4) L (p^2/f^2) \qquad (3)$$

where pupil diameter p = 1.707 mm and effective focal length f = 2 mm. Since the transmittance of the mouse eye (τ) for blue spectrum is approximately 86%, we obtain $\pi\tau/4 = 0.68$. The minimal source radiance L required for retinal irradiance I is calculated to be L = 70I. This means to achieve the threshold retinal irradiance of 0.05mW/mm^2, a source with radiance L = 3.5 mW/(mm^{2}sr) is required. For our case, the power reaching the retina (P_r) is 2.23 mW when the source fiber is at a distance of 2 mm from the eye. From the area of the receiving fiber (core diameter: 200μm), the power received by the fiber was calculated to be 89μW.

3.2. Simulation of intensity distribution maps at varying distances of excitation source from the eye

Zemax modeling of the eye was done in the sequential mode. Details about the simulation method are described in materials and methods. For each surface in the mouse eye, the parameters like the radius of curvature, thickness, semi diameter and the refractive indices etc were input following references[22-25]. The spot diagrams are set for 20 rays and the irradiance map is obtained by the physical optics propagation. The spot diagram and irradiance map for the diverging fiber source at different distances from the mouse cornea is shown in Figure 2. Table 2 summarizes the simulation results for peak irradiance and total power obtained on the mouse retina for varying source distances.

Source Distance (mm)	Peak Irradiance at Retina (mW/mm^2)	Total Power at the Retina (mW)
3	0.0688	0.15
4	0.0923	0.086160
5	0.3605	0.022145

Table 2: Summary of the simulation results for peak irradiance and power obtained on the mouse retina for varying source distances.
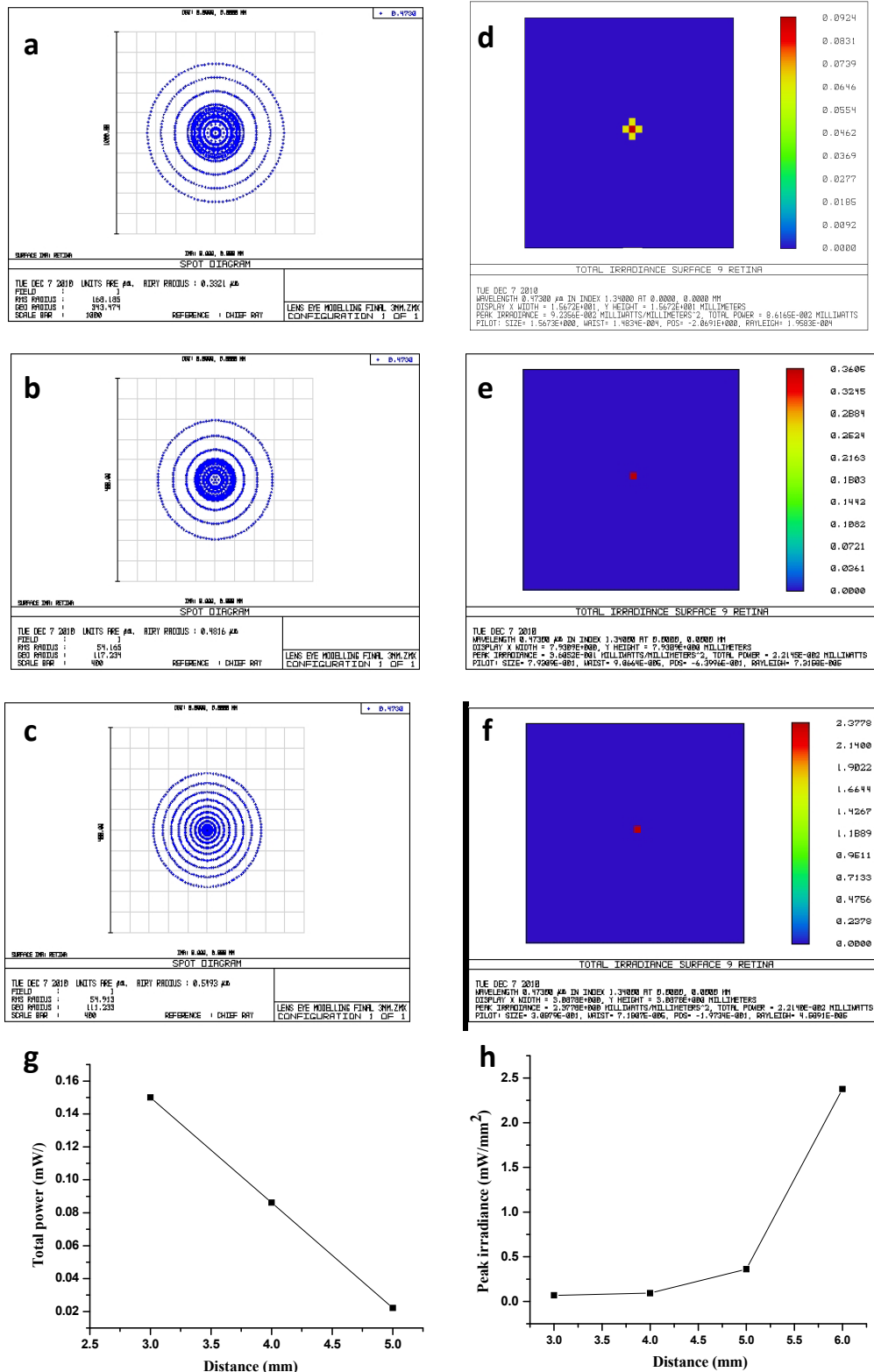
Figure 2: Spot diagram at retina for source distance of (a) 4mm, (b) 5mm and (c) 6 mm from the mouse retina. The total irradiance pattern on the surface of the retina for source distance of (d) 4mm, (e) 4mm and (f) 6 mm. (g) Total power output and (h) Peak irradiance reaching the retina of mouse eye being irradiated at varying distances using a diverging optical fiber source.

The total irradiance pattern on the surface of the retina for varying source distance is shown in Figure 2d to f. As shown in Figure 2g, though the total power reaching the retina decreases at larger distance of the source fiber, the peak irradiance increases (Figure 2h). This can be attributed to the fact that some light is lost at larger source distance due to finite size of the collecting eye-optics and the pupil size. However, the imaging spot size decreases significantly as seen in Figures 2b to c when the source distance is increased from 2mm to 3mm. These two effects counter-acts leading to the obtained peak irradiance pattern (Figure 2h). While peak irradiance is important for generating action potential, the spot size at retina will determine the spatial resolution. However, the total power, transmitted up to the retina, covering one cell is important for overall stimulation efficiency. Therefore, for design of retinal prosthesis or even in experimental settings, these parameters need to be optimized in order to find desired effect while using optogenetic stimulation.

3.3. Experimentally obtained power transmission mappings

In order to estimate the actual power reaching the retina, power measurements were carried out in dark-adapted mice eye, illuminated with diverging light from an optical fiber (200 μm core) and power measured from the receiving fiber (200μm core) inserted through the back of the eye up to retina via a guiding needle. Figure 3 shows normalized power measured at the receiver fiber end with varying distances from the source fiber.
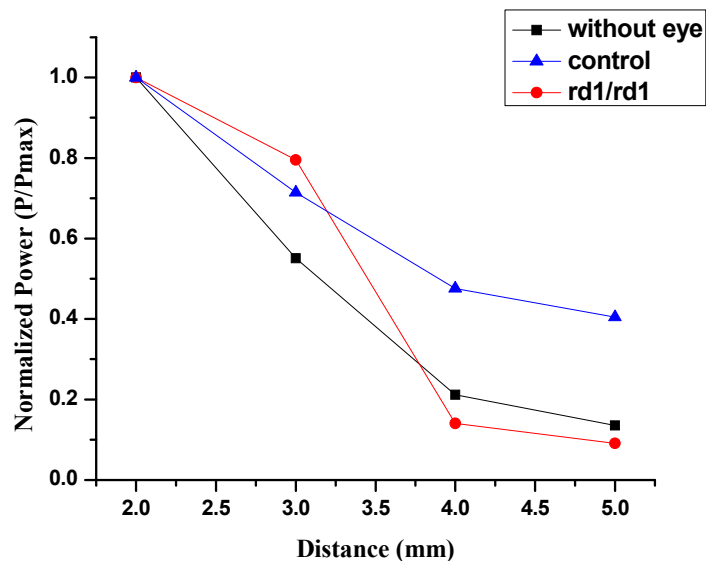

Figure 3: Normalized power measured at varying distances from the source fiber. Symbol (-■-) denotes measurements without placing an eye in between the source and receiver fiber, symbol (-▲-) denotes the condition where eye of control mouse is in between the two fibers and symbol (-●-) denotes the condition where eye of rd1/rd1 mouse is in between the two fibers.

For both control (Figure 3a) and *rd1/rd1* mice (Figure 3b), placing eye in between the source and receiver fiber led to less steeper decrease in received power as a function of source-distance. This can be attributed to the fact that eye-optics acting as a condenser in collecting the diverging light from the source and focusing back on to the receiving fiber It can be noted that the decrease in measured power is ~2.5 times when the source fiber is moved 2 to 5 mm, while the theoretical simulations (Figure 2g) based on physical optics propagation shows a decrease of ~7.5 times for similar source-receiver distance. This discrepancy can be attributed to the fact that the peak irradiance increased (Figure 2h) with increasing source distance. Since, the receiving fiber has finite core size and acceptance angle, it cannot receive the total power reaching retina and therefore cannot exactly match the theoretical simulations (Figure 2g).

3.4. Effect of improved light sensitivity of the retina on mouse behavior in water maze

To determine restoration of vision in ChR2-transfected mice, one week after injection of plasmids, mice were tested with radial arm water maze[19]. Details of the maze are described in materials and methods section. Every time the

mouse was put close to the center of the maze, the platform was changed from the end of one arm to another. The above procedure was executed each day and as an award, each time after mouse arrived at the platform; it was transferred back to the cage for at least 20 min before the next test. After training for one week, the performance of the mouse was recorded. Figure 4a & b respectively show the representative track of *rd1/rd1* mice without or with Thy1-ChR2-YFP transfected retina. The mice transfected with the ChR2-genes performed significantly better, in response to optimally designed light source, than the mice without ChR2-expression. As shown in Figure 4c, the mean number of arms swam by the transfected mice before they reached the platform is significantly smaller than that of the mice without transfection (3.10 ± 0.88, n=6 for ChR2-transfected group vs. 1.00 ± 0.46, n=6 for r*d1/rd1* mice without injection, p<0.01). In consistence with the number of error arms, the distances (Figure 4d) and time (Figure 4e) traveled by the ChR2-transfected mice before arriving at the platform were much shorter than the *rd1/rd1* mice without transfection (230.67 ± 53.84 vs. 565.74 ± 112.97, and 63.60 ±11.12 vs. 25.80 ± 3.08, respectively, n=6 for both groups, p<0.01). Interestingly, the *rd1/rd1* mice rotated their head more frequently than the transfected mice (1.31 ± 0.49 for rd1/rd1 mice without transfection vs. 0.58 ± 0.22 for transfected mice, n=6, p<0.05) as shown in Figure 4f. This can be attributed to the hypothesis that the transfected mice could sense the laser beam, leading them to rotate their head until they felt the light source, while the *rd1/rd1* mice rotated its head randomly.
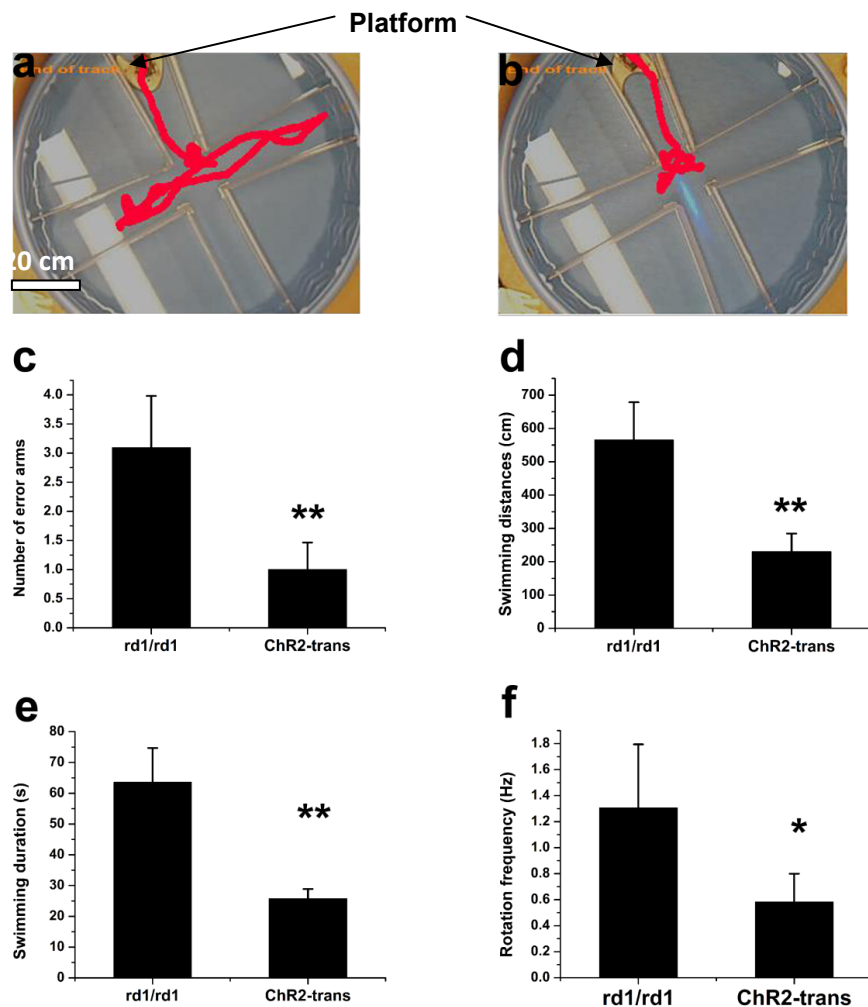

Figure 4: Mice transfected with ChR2 in eyes performed much better, in response to optimally-designed light source, than mice without transfection. Representative track of *rd1/rd1* mouse (a) without and (b) with Thy1-ChR2 transfected eyes. (c) Numbers of error arms mice swam before arriving at the platform; (d) swimming distance before reaching the platform; (e) swimming duration before finding the platform; (f) rotation frequency of mice head during swimming.

Inside the water maze, the platform acts as a reward system to mice that are constantly swimming since they can rest instead of having to swim. Mice with ChR2-transfected eyes performed significantly better than the mice without transfection and performance of ChR2-transfected mice in water maze was found to be quite stable in self-comparable group. Further, to evaluate the effect of stimulation intensity on ability of ChR2-treated mice, the mouse was placed at various distances along the beam path in order to find out the threshold light intensity. The behavior of the treated mice was found to depend on the intensity of the activating light with a threshold intensity (or distance) from where treated mouse could respond to the light. Since the laser light was made divergent, the intensity of light decreases away from the source. The stimulation intensity at different distances from the source correlated well with the mouse swimming score. Since the area of laser beam at the center of water maze was 40cm, according to Eq (2) and (3), the solid angle (Φ) of laser beam was $\Phi = A_P/r^2 = 0.000014$ and the radiance (L) of laser was $L = P_0/ (\Phi\ A_s\ \cos\theta) = 1012.8$ mW/(mm^{2}sr). It may be noted that upper bound source radiance of 700 mW/(mm^{2}sr) at 470 nm is estimated (section 3.1) for activating retinal neurons expressing ChR2. This is significantly higher than the ambient light and the laser radiance applied in our experiment is above this value. However, several factors need to be considered for delivering the threshold intensity at retina. For example, though our calculations took scattering (Fresnel reflection) losses due to refractive index mismatch of various layers of eye, it does not account for the loss of blue light (460 nm, the activation peak of ChR2) due to absorption[26] and point scattering centers. Further, various aberrations[27] needs to be considered in the model in order to evaluate the image quality[28] of optogenetically stimulated retina.

4. CONCLUSIONS

Stimulation of retinal neuronal cells using optogenetics via use of chanelrhodopsin-2 and blue light has opened up a new direction for restoration of vision with respect to treatment of *Retinitis pigmentosa*. In addition to delivery of ChR2 to specific retinal layer using genetic engineering, threshold level of blue light needs to be delivered onto the retina for generating action potential and successful behavioral outcome. In contrast to earlier viral method based delivery of ChR2 onto retinal ganglion cells, we successfully demonstrated *in-vivo* electroporation of RP mice eye and improved behavior subsequent to ChR2 transfection. Our simulations and measurement of intensity distribution of light reaching the retina of RP mouse models showed optimal divergence and distance of the stimulating source is required for efficient delivery of the light on to the retina. Further, the spot size at retina, contributing to the spatial resolution in optogenetically restored vision, was found to depend on the source positioning. The behavioral improvement in mice with ChR2 transfected retina was found to correlate with the stimulation intensity reaching the retina.

References

[1]   Sugawara, T., Hagiwara, A., Hiramatsu, A., Ogata, K., Mitamura, Y. and Yamamoto, S., "Relationship between peripheral visual field loss and vision-related quality of life in patients with retinitis pigmentosa", *Eye*, advance online publication, 24, 535-539 (2009).
[2]   Hartong, D. T., Berson, E. L. and Dryja, T. P., "Retinitis Pigmentosa", *Lancet* 368, 1795-809 (2006).
[3]   Stephen, D. P., Sara, B. J. and Lori, S. S., "Perspective on genes and mutations causing retinitis pigmentosa." *Arch Ophtalmology* 125, 151-58 (2007).
[4]   Mezer, E., Babul-Hirji, R., Wise, R., Chipman, M., DaSilva, L., Rowell, M., Thackray, R., Schuman, C. T. and Levin, A. V., "Attitudes regarding predictive testing for retinitis pigmentosa," *Opthal. Genet.,* 28, 9-15 (2007).
[5]   Hamel, C., "Retinitis Pigmentosa", *Orphanet Encyclopedia* 1-9 (2003).
[6]   Chow, A. Y., Pardue, M. T. Perlman, J. I. , , Ball, S. L., Chow, V.Y., Hetling, J. R., Peyman, G. A., Liang, C., Stubbs, Jr., E. B. and Peachey, N. S., "Subretinal implantation of semiconductor-based photodiodes: durability of novel implant designs", J. Rehabilit. Develop. 39, 313-322 (2002).
[7]   Zrenner, E., "Will Retina Implants Restore Vision ?" Science, 295, 1022-025 (2002).
[8]   Hossain, P., Seetho, I. W., Browning, A. C. and Amoaku, W. M., "Artificial means for restoring vision." British Med., J. 330, 30-33 (2005).

[9] Nagel, G., Szellas, T., Huhn, W, Kateriya, S, Adesishvili, N., Berthold, P., Ollig, D., Hegemann, P. and Bamberg, E., "Channelrhodopsin-2, a directly light-gated cation-selective membrane channel", Proc. Natl. Acad. Sci. USA, 100, 13940-13945 (2003).

[10] Boyden, E.S., Zhang, F., Bamberg, E., Nagel, G. and Deisseroth, K., "Millisecond-timescale, genetically targeted optical control of neural activity", Nat. Neurosci. 8, 1263-1268 (2005).

[11] Zhang, F. Wang, L., Boyden, E. S. and Deisseroth, K., "Channelrhodopsin-2 and optical control of excitable cells", Nat. Meth. 3, 785-792 (2006).

[12] Miller, G., "Shining new light on neural circuits", Science 314, 1674-1676 (2006).

[13] Nagel, G., Szellas, T., Huhn, W., Kateriya, S., Adeishvili, N., Berthold, P., Ollig, D., Hegemann, P.and Bamberg, E., "Light activation of channelrhodopsin-2 in excitable cells of Caenorhabditis elegans triggers rapid behavioral responses", Curr. Biol. 15, 2279-2284 (2005).

[14] Schroll, C., Riemensperger, T., Bucher, D., Ehmer, J., Voller, T., Erbguth, K., Gerber, B., Hendel, T., Nagel, G., Buchner, E. and Fiala, A., "Light-induced activation of distinct modulatory neurons triggers appetitive or aversive learning in Drosophila larvae", Curr. Biol. 16, 1741-1747 (2006).

[15] Bi, A., Cui, J., Ma, Y.P., Olshevskaya, E., Pu, M., Dizhoor, A.M. and Pan, Z.-H. "Ectopic expression of a microbial- type rhodopsin restores visual responses in mice with photoreceptor degeneration", Neuron 50, 23–33 (2006).

[16] Thyagarajan, S., van Wyk, M., Lehmann, K., Löwel, S., Feng, G. and Wässle, H., "Visual Function in Mice with photoreceptor degeneration and transgenic expression of channelrhodopsin 2 in Ganglion Cells", J. Neurosc. 30, 8745-8758 (2010).

[17] Tomita, H. Sugano, E., Isago, H., Hiroi, T., Wang, Z., Ohta, E. and Tamai, M., "Channelrhodopsin-2 gene transduced into retinal ganglion cells restores functional vision in genetically blind rats", Exp Eye Res. 90, 429-36 (2010).

[18] Lagali, P. S., Balya, D., Awatramani, G. B. ,, Munch, T. A.,Kim, D. S., Busskamp, V., Cepko, C. L. and Roska, B., "Light-activated channels targeted to ON bipolar cells restore visual function in retinal degeneration". Nat. Neurosci. 11, 667–75 (2008).

[19] Hodges, H., "Maze procedures: the radial-arm and water maze compared.", Cogn. Brain Res., 3: 167-181 (1996).

[20] Grossman, N., Nikolica, K., Poherd, V. and McGovern B., "Photostimulator for Optogenetic Retinal Prosthesis", IEEE EMBS Conf. Neural Engg., 68-71 (2009).

[21] Pennesi, M. E., Lyubarsky, A. L. andPugh, Jr, E. N., "Extreme responsiveness of the pupil of the dark-adapted mouse to steady retinal illumination", Invest. Ophthalmol. Visual Sc., 39 (1998).

[22] Lei, B.and Yao, G., "Spectral attenuation of the mouse, rat, pig and human lenses from wavelengths 360 nm to 1020 nm", Expt. Eye Res. 83, 610e614 (2006).

[23] Henriksson, J. T. and McDermott, A. M. "Dimensions and morphology of the cornea in three strains of mice", Invest. Ophthalmol. Vis. Sci. 50, 3648–3654 (2009).

[24] Remnlla, S. and Hallett, P. E., "A schematic eye for the mouse and comparisons with the rat", Vision Res. 25, 21- 31 (1985).

[25] Schmucker, C. and Schaeffel, F. "A paraxial schematic eye model for the growing C57BL/6 mouse", Vision Res. 44, 1857–1867 (2004).

[26] Dillon, J., Zheng, L., Merriam J. C. and Gaillard, E. R., "Transmission spectra of light to the mammalian retina", *Photochem. Photobiol.* 71 225-229 (2000).

[27] García de la Cera, E., Rodríguez, G. Llorente, L., Schaeffel, F. and Marcos S., "Optical aberrations in the mouse eye", Vision Res. 46, 2546–2553 (2006).

[28] Li, G., Zwick, H., Stuck, B. and Lund, D. J. "On the use of schematic eye models to estimate retinal image quality", J. Biomed. Opt., 5, 307–314 (2000).